SLAC-PUB-1051
May 1972

EFFECTS OF UNITARITY ON THE MULTIPERIPHERAL MODEL*

S. Auerbach, R. Aviv and R. Sugar

Department of Physics
University of California
Santa Barbara, California 93106

and

R. Blankenbecler

Stanford Linear Accelerator Center
Stanford University, Stanford, California 94305

ABSTRACT

Two models are presented for which the full multiparticle S-matrix is unitary at high energies. The production mechanism is based on the multiperipheral model. It is shown that the elastic scattering amplitude contains a new type of cut in the angular momentum plane which is dynamical in origin. This unitarity cut plays a crucial role in enforcing the Froissart bound. The contribution of the multiregge region of phase space to the total cross section is suppressed and decreases as a power of the energy in almost all situations. Inclusive cross sections have been discussed, but only elastic scattering will be treated here.

(Submitted to Phys. Rev. Letters.)

(An expanded version of this paper is available as SLAC-PUB-1047, which was submitted to Phys. Rev.)

*Work supported in part by the U. S. Atomic Energy Commission and the National Science Foundation.

In order to construct a realistic model of diffraction scattering and particle production at high energies it is necessary to take into account the constraints of multiparticle unitarity. In this note we discuss two models for which the full multiparticle S-matrix is unitary at high energies.[1] The production mechanism is similar to that of the multiperipheral model to the extent that secondary particles are created and destroyed from chains which are in turn exchanged between the high energy primary particles. However, in order for the models to satisfy unitarity, it is essential to take into account diagrams in which the secondaries are produced or destroyed from more than one chain. This means that the elastic scattering amplitude will have contributions from checkerboard diagrams such as the one shown in Fig. 1b as well as from the familiar ladder diagrams of Fig. 1a.

The most striking new feature of these models is the mechanism by which the Froissart bound is enforced. The sum of the checkerboard graphs, whose presence is required by unitarity, gives rise to a square root branch cut in the angular momentum plane. It should be emphasized that this unitarity cut is dynamical in origin as opposed to the almost kinematical origin of the familiar Mandelstam cuts, which are also present here, and the AFS cuts. The unitarity cut is not present in any individual diagram. It is associated with a divergence in the perturbation series for the S-matrix.

As is well known, the standard multiperipheral and multiregge models do not have the constraints of unitarity built in. As a result, they can give rise to a violation of the Froissart bound by having a regge pole to the right of $\ell=1$.[2] In the present case it is also possible for the ladder graphs to generate a pole to the right of $\ell=1$. However, in our solvable model we find that any pole which passes $\ell=1$ is always on an unphysical sheet because it has passed through the unitarity cut. Thus it is not possible to violate the Froissart bound.[3,4]

In addition to enforcing this bound, the unitarity cut tends to decrease the importance of the multiregge region of phase space. For most values of the input parameters in our models, the multiregge region yields a small energy decreasing contribution to the total cross section. In our solvable model the leading ℓ-plane singularity arising from the multiregge region can reach unity only if the input pole is itself greater than one. In this situation the Froissart bound can be saturated.

Let us now turn to the specification of the models to be discussed here. Two types of particles appear in our models. All states contain two nonidentical, spinless "nucleons", plus an arbitrary number of identical "pions". The pions can be created and destroyed, but not the nucleons. As in the eikonal model, it is assumed that the nucleons retain a large fraction of their longitudinal momenta throughout the scattering process.[5] Working in the center-of-mass, we take the S-matrix elements to be a function of Y, the rapidity difference between the nucleons; B, the transverse distance between the nucleons; and q_i and y_i, the transverse momentum and rapidity of the ith pion. In the eikonal approximation, the S-matrix is diagonal in Y and B. Our model is now completely specified by giving the amplitude for the production of n pions off a single chain, $W_n(Y,B;q_1,y_1,\ldots,q_n,y_n)$. By crossing symmetry W_n also describes chains in which some or all of the pions are incoming. It is convenient to introduce a single operator, Z_n, which handles all possible production and absorption processes involving n pions which is regulated by W_n in the following form,

$$Z_n(Y,\underset{\sim}{B}) = \frac{1}{2s}\int \prod_{i=1}^{n} dq_i \frac{1}{n!} W_n(Y,\underset{\sim}{B};\ldots) : \prod_{i=1}^{n}\left[a(\underset{\sim}{q}_i,y_i)+a^+(-\underset{\sim}{q}_i,y_i)\right] : ; \qquad (1)$$

where a and a^+ are the pion creation and annihilation operators normalized such that $[a',a^+] = 2(2\pi)^3\delta^2(\underset{\sim}{q}-\underset{\sim}{q}')\,\delta(y-y')$. The invariant phase space element is $dq \equiv d^2\underset{\sim}{q}\,dy/2(2\pi)^3$, and $s \equiv m^2e^Y$, where m is the nucleon mass. The creation

and annihilation operators have been normal ordered in Eq. (1) to prevent a pion from being reabsorbed on the same chain from which it was emitted. Since we wish to consider chains from which an arbitrary number of pions are created or destroyed, we introduce a hermitian operator and unitary S-matrix by

$$Z(Y,\underset{\sim}{B}) = \sum_{n=0}^{\infty} Z_n(Y,\underset{\sim}{B}) \quad , \qquad S(Y,\underset{\sim}{B}) = e^{iZ(Y,\underset{\sim}{B})} = \sum_{N=0}^{\infty} \frac{i^N}{N!} Z^N \quad . \tag{2}$$

Let us start by considering a model which is simple enough to be solved exactly. We take the exchange mechanism between adjacent particles on the chain to be that of a fixed pole, and ignore correlations between transverse momenta. The rapidities are taken to be strongly ordered. Working in the center-of-mass, we then write[6]

$$\frac{1}{2s} W_n(Y,\underset{\sim}{B};\underset{\sim}{q}_1,y_1,\ldots,\underset{\sim}{q}_n,y_n) = e^{-Y} f(\underset{\sim}{B}) \prod_{i=0}^{n} e^{\alpha(y_i-y_{i+1})} \theta(y_i-y_{i+1}) \prod_{j=1}^{n} g(\underset{\sim}{q}_j) \, , \tag{3}$$

where $y_0 = -y_{n+1} = \frac{1}{2} Y$. It is convenient to introduce creation and annihilation operators, c^+ and c, defined by

$$c = [\lambda Y]^{-1/2} \int \frac{d^2q}{(2\pi)^2} \int \frac{dy}{4\pi} \, g(\underset{\sim}{q}) \, a(\underset{\sim}{q},y) \, ,$$

where the effective coupling constant λ is chosen so that $[c,c^+] = 1$. $Z(Y,B)$ and $S(Y,B)$ can now be expressed in terms of the coordinate operator $X = \frac{1}{\sqrt{2}}(c+c^+)$,

$$Z(Y,B;X) = f(B) \exp\left[\left(\alpha - 1 - \frac{1}{2}\lambda\right) Y + (2\lambda Y)^{1/2} X\right] \, .$$

Clearly S is diagonal in this coordinate representation. We shall be primarily interested in elastic scattering, so the matrix element of S is needed between states

with no pions:

$$<0 \mid S(Y, \underset{\sim}{B}) \mid 0> = 1 + \frac{i}{2s} M_{22}(Y, \underset{\sim}{B}) = \frac{1}{\pi^{1/2}} \int_{-\infty}^{\infty} dx\, e^{-x^2} \exp iZ(Y, B; x), \quad (4)$$

where M_{22} is the elastic scattering amplitude.

It is instructive to examine M_{22} in the angular momentum plane[7]:

$$\int_0^{\infty} dY\, e^{-\ell Y} M_{22}(Y, \underset{\sim}{B}) = 2\, im^2 \left[(\ell-1)^{-1} - G(\ell)\, (-if(B))^{h(\ell)} + C(\ell, \underset{\sim}{B}) \right], \quad (5)$$

where

$$G(\ell) = \Gamma \left[(2/\lambda)^{1/2} \left((\ell-\alpha_c)^{1/2} - (1-\alpha_c)^{1/2} \right) \right] / \left[2\lambda(\ell-\alpha_0) \right]^{1/2}$$

$$h(\ell) = (2/\lambda)^{1/2} \left[(1-\alpha_c)^{1/2} - (\ell-\alpha_0)^{1/2} \right],$$

and $C(\ell, \underset{\sim}{B})$ is an entire function of ℓ for all values of B provided $\alpha < 1 + \frac{1}{2}\lambda$. If $\alpha > 1 + \frac{1}{2}\lambda$, then

$$M_{22}(\ell, B) = 2\, im^2 (\ell-1)^{-1} \left[-if(B) \right]^{h(\ell)} + C'(\ell, B), \quad (6)$$

where $C'(\ell, B)$ has only a branch point in ℓ at α_c. The position of this new dynamical cut is $\alpha_c = \alpha - \left(1-\alpha-\frac{1}{2}\lambda\right)^2 / 2\lambda$ for any value of α.

Figure 2 illustrates the ℓ-plane structure for the case $\alpha \leq 1 + \frac{1}{2}\lambda$. The N-Reggeon exchange amplitude has a pole at $\alpha(N) = 1 + N(\alpha-1) + \frac{1}{2}\lambda N(N-1)$. The pole at $\ell = \alpha(1) = \alpha$ is due to the exchange of a single fixed input pole. The pole at $\alpha(2) = 2\alpha - 1 + \lambda$ arises from the ladder graphs, and the poles with $N \geq 3$ from the checkerboard graphs with N vertical lines. In general, $<0 \mid Z^N \mid 0> = f^N(B) \exp Y\alpha(N)$, so that the series expansion of S given in Eq. (2) diverges. The poles with $N \geq 2$ are dynamical in origin and the quadratic dependence of $\alpha(N)$ is due to the fact that the number of attractive pairwise interactions increases as $N(N-1)/2$. The square root branch point at $\ell = \alpha_c$ is directly related to the above divergence of the perturbation expansion. Notice that $\alpha_c \leq 1$ for all values of λ and α. The only poles

on the physical sheet are those for which $N \leq \bar{N} = \left(1-\alpha+\frac{1}{2}\lambda\right)/\lambda$. Let us imagine that the coupling constant is increased from zero to infinity at a fixed value of $\alpha \leq 1$. For small values of λ the branch point is far to the left in the ℓ-plane. As λ is increased the dynamical poles move to the right, but the branch point moves even faster. Each pole eventually collides with the branch point and then moves off onto the unphysical sheet. At $\lambda = 2(1-\alpha)$ the branch point circles the fixed pole and starts to retreat back to the left. Therefore, for $\lambda > 2(1-\alpha)$ the branch point is the only singularity on the physical sheet.

The behavior of the cross section as the parameters are varied is now easy to follow. The total cross section is dominated by the dynamical pole arising from the ladder graphs as long as this singularity is on the physical sheet. We thus have $\sigma_T(s) \sim (s/m^2)^{2\alpha-2+\lambda}$ for $\lambda \leq \frac{2}{3}(1-\alpha)$. On the other hand, for $\lambda > \frac{2}{3}(1-\alpha)$ the branch point dominates and we then find $\sigma_T(s) \sim (s/m^2)^{\alpha_c - 1}\left[\ell n(s/m^2)\right]^{-1/2}$. Thus for $\alpha < 1+\frac{1}{2}\lambda$ the total cross section always goes to zero at high energies. This includes the case $\alpha=1$, which is given above with $\alpha_c = -\lambda/8$.

For $\alpha > 1+\frac{1}{2}\lambda$ the scattering amplitude has a branch point at $\ell=\alpha_c$ and an additional singularity at $\ell=1$. To illuminate the form of this singularity we make the particular choice $f(\underset{\sim}{B}) = e^{-B/R}$. Then the Fourier transform with respect to B gives

$$M_{22}(\ell, \underset{\sim}{\Delta}) = 2\,\mathrm{im}^2 R_0^2 \left[(\ell-1)^2 + R_0^2 \underset{\sim}{\Delta}^2\right]^{-3/2} + c(\ell, \underset{\sim}{\Delta}) \quad , \tag{7}$$

where $R_0 = R\left(1-\alpha+\frac{1}{2}\lambda\right)$ and $c(\ell, \underset{\sim}{\Delta})$ has only the branch point at $\ell=\alpha_c$. The two-dimensional momentum transfer is Δ, and at high energies, $t \simeq -\underset{\sim}{\Delta}^2$. The first term in Eq. (15) is just the ℓ-plane singularity associated with scattering from a black disc of radius R_0Y.[4] It gives rise to a total cross section of the form $\sigma_T(s) = 2\pi R_0^2\left[\ell n\, s/m^2\right]^2$. If one increases α for fixed λ, the square root branch points at $\ell = 1 \pm i R_0\sqrt{-t}$ enter the physical sheet through the unitarity cut when

$\alpha = 1 + \frac{1}{2}\lambda$. At this point $\alpha_c = 1$, and $R_0 = 0$. Notice that for sufficiently large values of λ the total cross section always goes to zero at high energies for fixed α.

The unitarity cut which we have exhibited explicitly in this solvable but quite general model, will be present in a wide class of multiperipheral-like models. To see this point, let us consider a form for W_n more closely related to the standard multiregge model:

$$W_n(Y, \underset{\sim}{\Delta}; \underset{\sim}{q}_1, y_1; \ldots \underset{\sim}{q}_n, y_n) = \prod_{i=1}^{n+1} \beta(\underset{\sim}{k}_i)\, e^{\alpha(\underset{\sim}{k}_i)x_i}\, \theta(x_i) \prod_{j=1}^{n} g(\underset{\sim}{k}_j, \underset{\sim}{k}_{j+1}) \,, \tag{8}$$

where $\underset{\sim}{\Delta}$ is the two-dimensional momentum conjugate to $\underset{\sim}{B}$, $\underset{\sim}{k}_i = \sum_{j=1}^{i+1} \underset{\sim}{q}_j$, and $x_i = y_i - y_{i+1}$. In the region of phase space in which all subenergies are large, this choice for W_n exactly reproduces the multiregge amplitude.

The present model cannot be solved analytically; however, it is possible to write down an integral equation for the amplitude $Z_N \equiv \langle 0 | Z^N | 0 \rangle$. A typical diagram contributing to Z_4 is shown in Fig. 1b. Clearly Z_N gives the contribution to the elastic scattering amplitude arising from N reggeon exchange. It is convenient to work in the ℓ-plane. We introduce the Green's function for the propagation of N free reggeons, $G_N(\ell)$, by

$$\langle \underset{\sim}{k}'_1 \ldots \underset{\sim}{k}'_N | G_N(\ell) | \underset{\sim}{k}_1 \ldots \underset{\sim}{k}_N \rangle = \prod_{i=1}^{N} (2\pi)^2 \delta^2(k_i - k'_i) \cdot \left[\sum_{i=1}^{N} \alpha(k_i) - \ell - N \right]^{-1} \,, \tag{9}$$

and the N reggeon potential , V_N, by

$$V_N = \sum_{i<j}^{N} V_{ij} \,, \tag{10}$$

where

$$\langle \underset{\sim}{k}'_1, \ldots \underset{\sim}{k}'_V | V_{ij} | \underset{\sim}{k}_1, \ldots \underset{\sim}{k}_N \rangle = - \prod_{\ell \neq i,j}^{N} (2\pi)^2 \delta^2(\underset{\sim}{k}_\ell - \underset{\sim}{k}'_\ell)$$

$$\cdot (2\pi)^2 \delta^2(\underset{\sim}{k}_i + \underset{\sim}{k}_j - \underset{\sim}{k}'_i - \underset{\sim}{k}'_j) \left[\beta(\underset{\sim}{k}_i)\beta(\underset{\sim}{k}'_i)\beta(\underset{\sim}{k}_j)\beta(\underset{\sim}{k}'_j) \right]^{1/2} \cdot \frac{1}{4\pi}\, g(\underset{\sim}{k}_i, \underset{\sim}{k}_j)\, g(\underset{\sim}{k}'_i, \underset{\sim}{k}'_j) \,.$$

If we take the input trajectory to be linear and write $\alpha(k) = \alpha - \alpha' k^2$, then the integral equation for Z_N is exactly analogous to the Lippman-Schwinger equation in two-dimensions.[8] The quantity that corresponds to the energy variable is $E_N = -\ell + N(\alpha - 1)$. Clearly, determining the position of the leading regge pole that contributes to Z_N is equivalent to solving for the ground state energy of a two-dimensional, N-body system. One expects that the residue function, $\beta(k)$, and the vertex function $g(k, k')$ will be regular at the origin and will go to zero for large values of their arguments. Since there are $\frac{1}{2} N(N-1)$ attractive potential energy terms and N repulsive kinetic energy terms in the Hamiltonian, one expects the binding energy of the ground state to grow like N^2. In other words, the leading regge pole should move to the right in the ℓ-plane as N^2. For a wide range of input functions, it is in fact possible to prove that the t=0 intercept of the leading pole has the form[1] $\alpha_N(0) = a(N) - bN + cN^2$, where c is a positive constant and a(N) is expected to go like a constant for large N. It follows at once that the series expansion for the S-matrix given in Eq. (4) diverges, just as it does for the solvable model.

It is convenient as well as necessary to introduce an alternative definition of the S-matrix by writing

$$S(Z) = \frac{1}{\pi^{1/2}} \int_{-\infty}^{\infty} dx\, e^{-x^2}\, \tilde{S}(Z\, e^{2dx}) , \tag{11}$$

where

$$\tilde{S}(Z) = \sum_{N=0}^{\infty} \frac{i^N}{N!} Z^N e^{-d^2 N^2} . \tag{12}$$

d is a real constant whose numerical value is at our disposal. When it is permissible to interchange the order of summation and integration, one recovers Eq. (2). However, even when this is not possible, one can show by formal manipulation that the S-matrix defined by Eqs. (11) and (12) is unitary.

It is now a simple matter to compute the contribution of the leading regge poles in Z_N to the elastic scattering amplitude. A particularly simple choice for d which guarantees the convergence of the series of Eq. (12) is $d=(cY)^{1/2}$. One finds that in the present model there are an infinite number of square root branch points in the ℓ-plane. At t=0 they are located at $\alpha_c(N) = a(N) - b^2/4c$. The ℓ-plane structure of the elastic amplitude is essentially the same as in the case of the solvable model. In particular the mechanism for avoiding violation of the Froissart bound is the same - the unitarity cut.

The point we wish to emphasize is that the mechanism for avoiding violation or saturation of the Froissart bound, discussed in these two rather single models, is likely to be present in a wide class of models. Unitarity requires that we take into account the checkerboard diagrams of Fig. 1b as well as the more familiar ladder diagrams. A simple counting argument then shows that the amplitudes Z_N will have poles arbitrarily far to the right in the ℓ-plane unless the forces between reggeons saturate. It is hard to see how these features could be changed in more sophisticated models that take into account low subenergy effects. Since the S-matrix is explicitly unitary, it cannot have ℓ-plane singularities in the physical sheet to the right of $\ell=1$. As a result, it must have branch cuts which are of a different type than those discussed by Mandelstam.[9] In our solvable model we find that if the input trajectory is one or less, the multiregge region of phase space provides a contribution to the total cross section that decreases as a power of the energy. Hence the experimentally observed constant total cross sections must arise from other sources, such as the fragmentation region or the low subenergy pionization region.

Figure Captions

1. Typical ladder (a) and checkerboard (b) graphs.
2. Analyticity in ℓ-plane. Dashed poles on unphysical sheet.

REFERENCES

1. A more detailed exposition of these models is given elsewhere. S. Auerbach, R. Aviv, R. Blankenbecler and R. Sugar, SLAC-PUB-1047.
2. J. Finkelstein and K. Kajante, Phys. Letters 26B, 305 (1968).
3. Recently several different approaches have been suggested for enforcing the Froissart bound when the ladder graphs have a singularity to the right of $\ell = 1$ (see reference 4). However, in these models the Froissart bound is saturated from the multiregge region of phase space. This result is unsatisfactory experimentally since particles produced at high energies tend to have rather low relative energies.
4. H. Cheng and T. T. Wu, Phys. Rev. Letters 25, 1586 (1970); J. Finkelstein and F. Zachariasen, Phys. Letters 34B, 631 (1971); J. R. Fulco and R. L. Sugar, Phys. Rev. D5, 1919 (1971).
5. Models of this type have been discussed recently by R. Aviv, R. Blankenbecler and R. Sugar, Phys. Rev. D. (to be published), and G. Calucci, R. Jengo and C. Reggi, Nuovo Cimento 4A, 330 (1971), 6A, 601 (1971), and to be published.
6. In order for the eikonal approximation to be valid one should introduce theta functions to the W_n which restrict the pion rapidities to the range $|y_i| \leq \frac{1}{2}(1-\epsilon)Y$ (see references 1 and 4). Since in most cases ϵ can be set equal to zero at the end of the calculation, we shall not write it explicitly.
7. A. Erdelyi et al., Tables of Integral Transforms, Vol. I, p. 146.
8. The reggeon calculus used here is in the spirit of that discussed by V. N. Gribov, Zh. Eksp. Teor. Fiz. 53, 654 (1967) [Sov. Physics JETP 28, 414 (1968)] and H. D. I. Abarbanel, NAL Preprint THY-28 (1972).
9. The amplitudes Z_N contain the Mandelstam cuts. In fact the regge poles enter the physical sheet of the Z_N through these cuts.

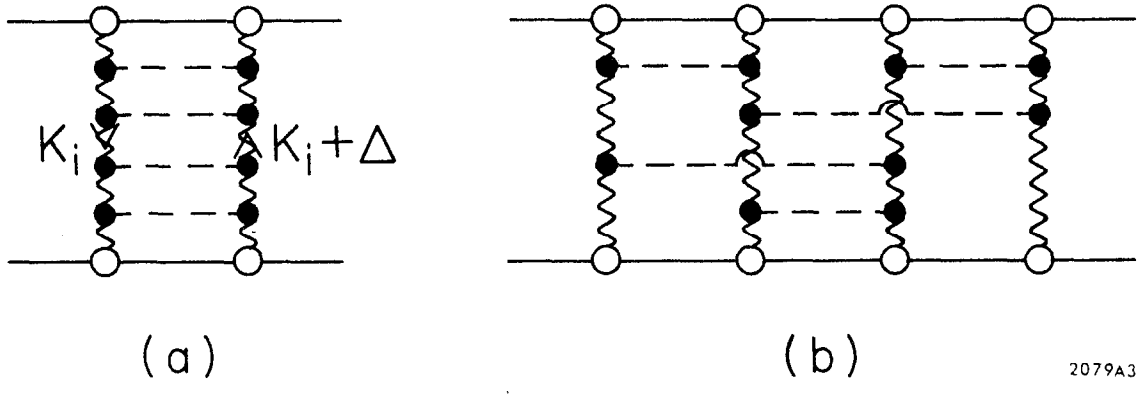

Fig. 1

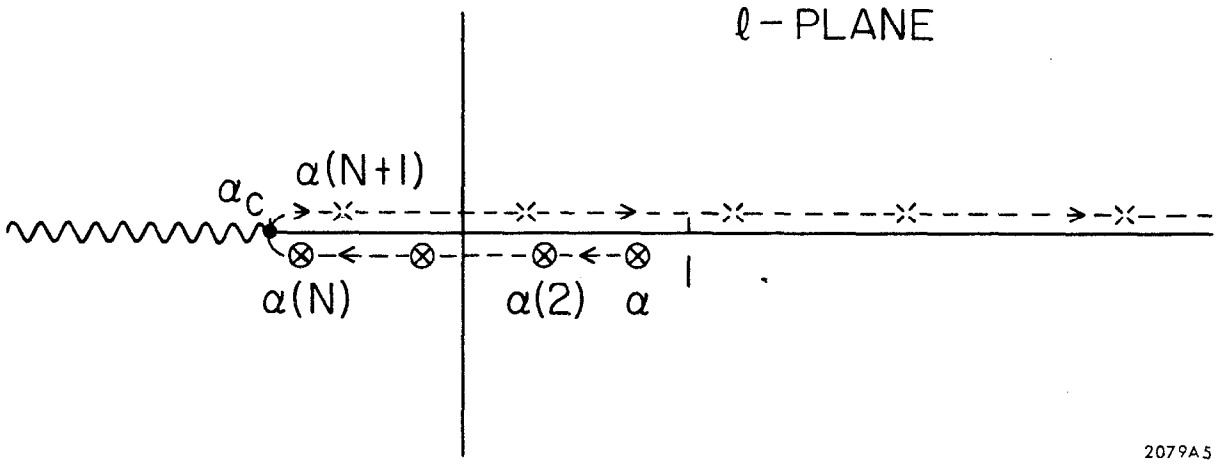

Fig. 2